

# Magneto-optical Kerr effect measurements under bipolar pulsed magnetic fields

Soichiro Yamane<sup>1\*</sup>, Sota Nakamura<sup>1</sup>, Atsutoshi Ikeda<sup>1</sup>,  
Kosuke Noda<sup>2</sup>, Akihiko Ikeda<sup>2</sup>, and Shingo Yonezawa<sup>1</sup>

<sup>1</sup>Department of Electronic Science and Engineering, Kyoto University, Kyoto 615-8510, Japan

<sup>2</sup>Department of Engineering Science, University of Electro-Communications, Tokyo 182-8585, Japan.

\* E-mail : yamane.soichiro.73f@st.kyoto-u.ac.jp

**Abstract.** The magneto-optical Kerr effect (MOKE) is a powerful probe of magnetism. Its contact-free optical nature makes it potentially well suitable for measurements under pulsed magnetic fields if various difficulties are overcome. In this paper, we report the establishment of MOKE measurements under bipolar pulsed magnetic fields up to 13.1 T. The accuracy of the setup was demonstrated by the excellent agreement with static-field results on the (001) surface of a  $\text{Fe}_3\text{O}_4$  single crystal. Furthermore, clear hysteresis loops of various commercial permanent magnets were successfully observed. The capability for rapid characterization of hysteretic properties highlights the versatility of our pulsed-field MOKE setup for both fundamental materials science and engineering applications.

## 1. Introduction

The magneto-optical Kerr effect (MOKE) is an optical probe of magnetism. In most materials, the Kerr angle ( $\theta_K$ ), rotation of the light's polarization, is proportional to magnetization. Consequently, ferromagnets such as iron exhibit relatively large  $\theta_K$  of the order of milliradians. Moreover, MOKE has enabled various discoveries in various materials beyond ferromagnets [1–3]. MOKE is therefore a key non-contact probe for exploring frontiers of materials science.

From an experimental viewpoint, because MOKE measurements requires no electrical contacts, it potentially well matches with pulsed magnetic fields. However, only a few MOKE studies under pulsed fields have been reported [4–6], owing to limited sample spaces in a pulse-field coil and small  $\theta_K$  in most materials. Despite these challenges, we recently succeeded in measuring  $\theta_K$  of various ferromagnetic or ferrimagnetic samples in pulsed fields exceeding 40 T and down to 77 K [7] using a portable pulse-field generator [8] and a zero-area-loop (loop-less) Sagnac interferometer [9]. This accomplishment is driven by our new compact sample fixture matching with a small bore of a coil and a phase-resolved numerical lock-in analysis for MOKE signals [7]. As a next step,

MOKE measurements in bipolar magnetic fields enable the observation of full magnetic hysteresis loops, which is indispensable for characterizing the coercivity and remnant magnetization of magnetic materials. These advances further establish pulsed-field MOKE as a promising approach in both fundamental and applied magnetism.

In this paper, we report successful MOKE measurements under bipolar pulsed magnetic fields up to 13.1 T. The validity and utility of our setup are demonstrated by results from  $\text{Fe}_3\text{O}_4$  and various permanent magnets.

## 2. Experimental methods

For MOKE measurements under bipolar pulsed magnetic fields, we used a method essentially the same as our previous work [7] for unipolar pulsed fields. From the interference signal detected by a photodetector and an oscilloscope,  $\theta_K$  is extracted via phase-resolved numerical lock-in analysis [7]. In this work, we newly developed a flexible command-line interface (CLI) tool for pulsed MOKE measurements [10]. This CLI, mainly built by the Rust programming language, provides efficient and user-friendly tools for analyzing large datasets obtained in pulsed-field MOKE measurements. For instance, the core numerical lock-in processing of 10 million data points is computed in less than 200 ms on a standard laptop. We used an integration time of  $\tau = 1.72 \mu\text{s}$  in our numerical lock-in analysis, and further smoothed the data using a moving average with a window size of 20 points (corresponding to 10.0  $\mu\text{s}$ ) to improve the signal-to-noise ratio.

Bipolar pulsed magnetic fields up to 13.1 T were generated using a portable pulse-field generator [8], which was modified by adding a diode antiparallel to the thyristor to allow a bipolar current oscillation of a single period. The magnetic field was measured by monitoring the current flowing through the main coil using a Rogowski sensor. The optical configuration of our polar MOKE setup was described in Ref. [7]; the incident and reflected lights are collinear to the field, and the positive direction of magnetic fields is defined as antiparallel to the incident light (Faraday geometry);  $\mathbf{H} \parallel -\mathbf{k}$ , where  $\mathbf{H}$  is the magnetic field and  $\mathbf{k}$  is the wave vector of the incident light. We also performed static-field MOKE measurements using a commercial superconducting magnet (Quantum Design, PPMS), employing the same optical geometry as the pulsed-field setup.

Demonstration of polar MOKE measurements in bipolar pulsed fields was conducted on the (001) surface of a commercial  $\text{Fe}_3\text{O}_4$  single crystal. Commercial permanent magnets made of various ferromagnetic materials were used to investigate the hysteretic magnetic properties.

## 3. Demonstration of bipolar pulsed-field MOKE measurements using $\text{Fe}_3\text{O}_4$

Figure 1 shows results of a MOKE measurement on a (001) surface of a  $\text{Fe}_3\text{O}_4$  single crystal under a bipolar pulsed magnetic field at room temperature. Figure 1(a) shows the time dependence of the magnetic field. After the field pulse is triggered, the magnetic field reaches 13.1 T at 0.7 ms, then decreases to  $-1.9$  T at 2.6 ms, and returns to

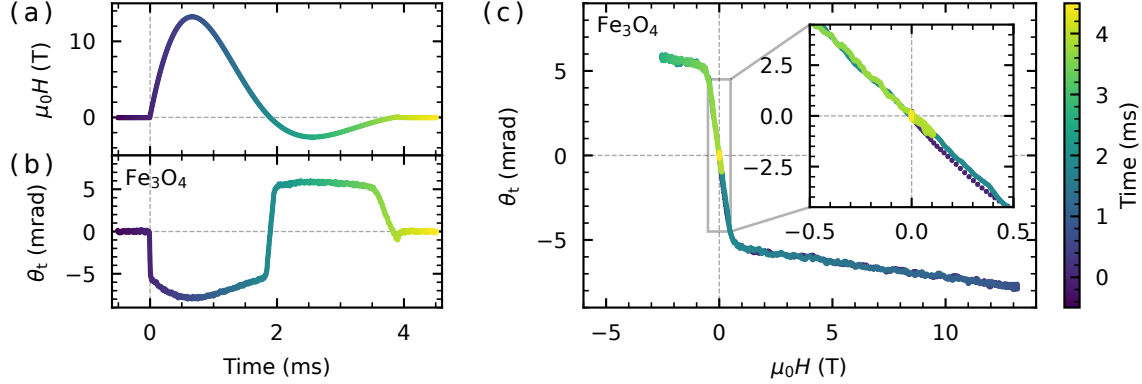


**Figure 1.** Results of MOKE measurements on the (001) surface of a  $\text{Fe}_3\text{O}_4$  single crystal under a bipolar pulsed magnetic field up to 13.1 T at room temperature. Time dependence of (a) the magnetic field and (b) the total magneto-optical (MO) angle. (c)  $\theta_t$  as a function of magnetic field. The inset shows a magnified view around zero magnetic field. For all panels, the color of data points indicate the time evolution from the beginning of the pulse, as shown in the colorbar on the right.

0 T at 4.0 ms. Figure 1(b) exhibits the time dependence of the total magneto-optical (MO) angle ( $\theta_t = \theta_K + \theta_{bg}$ ), where  $\theta_{bg}$  is a background mainly originating from the Faraday effect of optical components. Upon applying the bipolar pulsed magnetic field,  $\theta_t$  clearly responds to the time profile of the magnetic field. The steep changes between  $\theta_t = \pm 5$  mrad are due to the alignment of ferrimagnetic domains in  $\text{Fe}_3\text{O}_4$ , whereas the gradual changes beyond  $\pm 5$  mrad are attributed to the background Faraday effect as discussed below. The magnetic-field dependence of  $\theta_t$  is plotted in Fig. 1(c). The inset magnifies the region around zero magnetic field. Within our experimental resolution, negligible hysteresis loop was observed, consistent with the known soft ferrimagnetic nature of  $\text{Fe}_3\text{O}_4$  at room temperature [11].

To extract  $\theta_K$  from the total angle  $\theta_t$ , the background Faraday rotation  $\theta_{bg} = \alpha H$  is subtracted as illustrated in the inset of Fig. 2. The proportionality constant  $\alpha$  is determined by fitting the data above 5 T to the function  $\theta_t(H) = \theta_K^{\text{sat}} + \alpha H$ , where  $\theta_K^{\text{sat}}$  denotes the saturated Kerr angle. Figure 2 shows the obtained  $\theta_K(H)$ . For comparison, the  $\theta_K$  measured in a static magnetic field using a commercial cryostat is also plotted. The two datasets show excellent agreement, validating the accuracy of our bipolar pulsed-field MOKE measurements, even under the challenging conditions of rapidly changing magnetic fields with only a duration of a few milliseconds.  $\theta_K^{\text{sat}}$  is evaluated to be  $-5.39 \pm 0.01$  mrad, which is close to the literature values at room temperature [12, 13], as summarized in Table 1. The small variations in  $\theta_K^{\text{sat}}$  can be attributed to differences in surface orientation and treatment, as well as the use of a broadband incoherent light source in our experimental setup. Overall, our MOKE measurements successfully capture the magnetization behavior of  $\text{Fe}_3\text{O}_4$ , demonstrating the effectiveness of our approach for studying magnetic materials under bipolar pulsed fields.

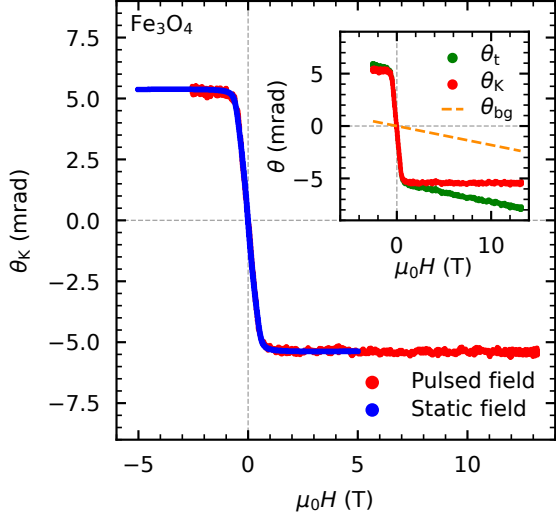


**Figure 2.**  $\theta_K(H)$  of a (001) surface of a  $\text{Fe}_3\text{O}_4$  single crystal at room temperature. Red points present results obtained in the bipolar pulsed magnetic field up to 13.1 T, while blue points show results measured in a static magnetic field. The inset describes the separation of  $\theta_K$  (red points) and  $\theta_{\text{bg}}$  (orange dashed line) from  $\theta_t$  (green points).

**Table 1.** Comparison of  $\theta_K^{\text{sat}}$  of  $\text{Fe}_3\text{O}_4$  at room temperature. All literature values were obtained at a photon energy of 0.8 eV (1550-nm wavelength).

$\theta_K^{\text{sat}}$ (mrad)	Surface Treatment	Field	Ref.
<b><math>-5.39 \pm 0.01</math></b>	<b>As-polished (001)</b>	<b>5 – 13.1 T</b>	<b>This work</b>
-5.14	Heat-treated (110)	1 T	[12]
-4.91	As-polished (110)	1 T	[12]
-4.36	Annealed (110)	1.76 T	[13]

#### 4. Bipolar pulsed-field MOKE measurements on various permanent magnets

Figure 3 displays results of MOKE measurements on (a) an alnico magnet (alnico5, material grade SAN52 [14]), (b) a neodymium magnet ( $\text{Nd}_2\text{Fe}_{14}\text{B}$ , material grade N52 [14]) with a Ni/Cu/Ni protective coating, and (c) a samarium-cobalt magnet ( $\text{Sm}_2\text{Co}_{17}$ , material grade SS28 [14]) under bipolar pulsed magnetic fields at room temperature. Clear hysteresis loops were observed in all samples, highlighting the capability of our bipolar pulsed-field MOKE setup to capture magnetic hysteresis and domain properties. We note that magnetic properties of the neodymium magnet were measured through its Ni/Cu/Ni coating. Thus the values of  $\theta_K$  originate from the coating layer, whereas the wide hysteresis captures the magnetic properties of the magnet. In engineering viewpoints, it is important that hysteretic properties be obtainable from as-bought samples without removing the coating. The Ni/Cu/Ni-coated  $\text{Nd}_2\text{Fe}_{14}\text{B}$  magnet exhibits a positive  $\theta_K$  at a positive field, in contrast to the other two magnets. This positive rotation is consistent with the known positive  $\theta_K$  of Ni at 0.8 eV under a positive magnetic field [15, 16].

To quantify properties as permanent magnets, characteristic fields ( $\mu_0 H_{\theta_K=0}$ ), where  $\theta_K$  becomes zero, were determined from the negative-field side of the hysteresis loops. This approach ensures reliable values, free from transient effects arising from the initial magnetization process near zero field and the rapid initial field-sweep rate. The obtained

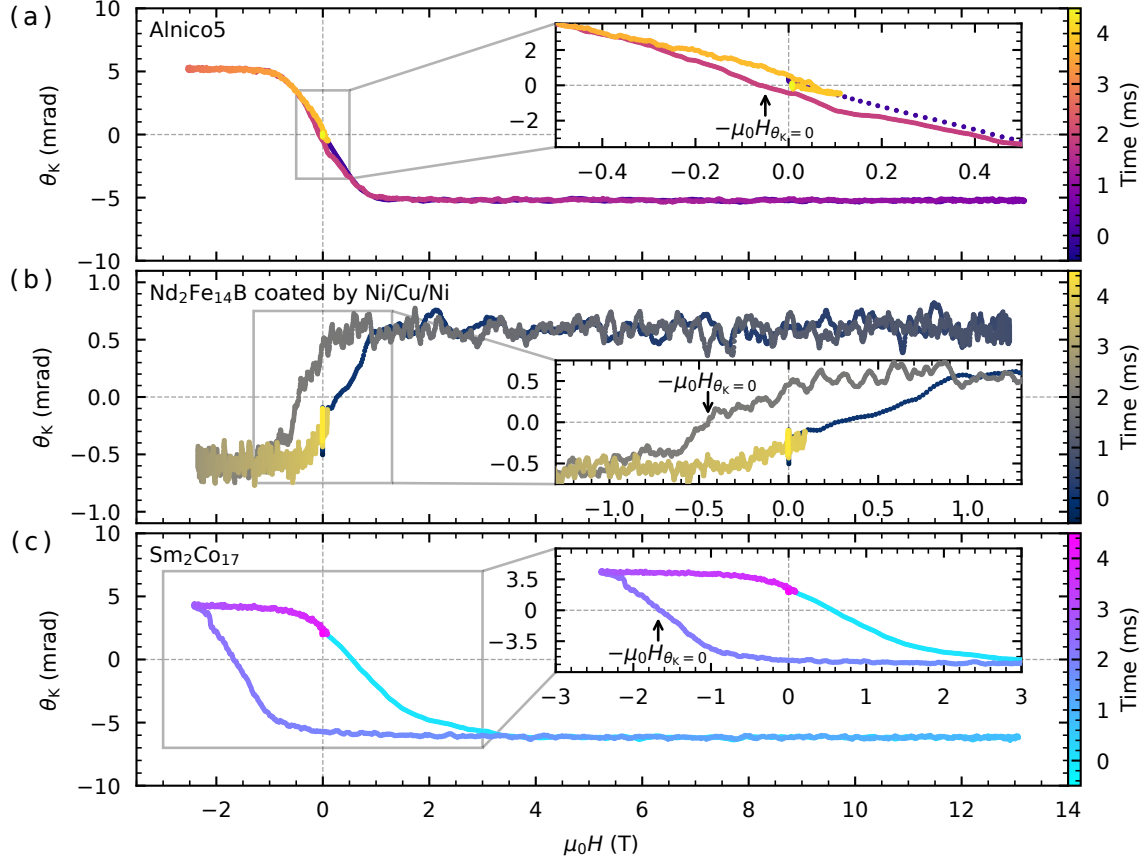


**Figure 3.** Results of MOKE measurements on various permanent magnets under bipolar pulsed magnetic fields at room temperature. Hysteresis loops of (a) alnico5, (b) Nd<sub>2</sub>Fe<sub>14</sub>B with a Ni/Cu/Ni protective coating, and (c) Sm<sub>2</sub>Co<sub>17</sub>. Because details of the starting trajectories vary depending on the magnetic history, we here plot representative data exhibiting largest hysteresises. We note that the overall hysteresis loop shapes themselves represent the intrinsic and reproducible properties of each magnet.

$\mu_0 H_{\theta_K=0}$  values are approximately (a) 0.05 T for the alnico5 magnet, (b) 0.45 T for the Nd<sub>2</sub>Fe<sub>14</sub>B magnet, and (c) 1.68 T for the Sm<sub>2</sub>Co<sub>17</sub> magnet. According to the supplier's datasheets [14], the standard intrinsic coercive fields ( $\mu_0 H_{cj}$ ) are (a) 0.07 T, (b)  $\geq 1.1$  T, and (c)  $\geq 1.8$  T, respectively. Thus, the measured  $\mu_0 H_{\theta_K=0}$  values are lower than the datasheet specifications for all samples. This fact can be attributed to the local probing nature of polar MOKE, which is primarily sensitive to the out-of-plane component of the local magnetization ( $\mathbf{M} \parallel \mathbf{k}$ ), and is insensitive to in-plane local magnetization ( $\mathbf{M} \perp \mathbf{k}$ ). When the magnetic field is close to  $\mu_0 H_{cj}$ , the magnetization reversal process involves the formation of magnetic domains with various orientations. In particular, near surfaces perpendicular to the external magnetic field, domains with in-plane magnetization should tend to be formed so that the stray field outside the sample is minimized. Consequently, the out-of-plane component of the magnetization within the light spot for MOKE measurements should decrease more rapidly than the total magnetization measured by bulk methods, resulting in  $H_{\theta_K=0}$  lower than  $H_{cj}$ .

## 5. Conclusion

We have successfully demonstrated MOKE measurements under bipolar pulsed magnetic fields up to 13.1 T at room temperature using a zero-area-loop Sagnac interferometer. Excellent agreement between pulsed-field and static-field MOKE measurements was achieved on the (001) surface of  $\text{Fe}_3\text{O}_4$ , validating the performance of our approach. The saturated  $\theta_K$  obtained from the pulsed experiment was  $-5.39 \pm 0.01$  mrad, close to literature values. Moreover, clear hysteresis loops were observed in various permanent magnets, alnico5, Ni/Cu/Ni-coated  $\text{Nd}_2\text{Fe}_{14}\text{B}$ , and  $\text{Sm}_2\text{Co}_{17}$ . The successful observation of distinct hysteresis loops establishes our bipolar pulsed-field MOKE setup as a versatile tool for both fundamental research and rapid characterization in applied magnetism, paving the way for future exploration of novel magnetic materials.

## Acknowledgments

This work was supported by Grant-in-Aids for Academic Transformation Area Research (A) "1000 Tesla Science" (KAKENHI Grant Nos. JP23H04859 and JP23H04861) from the Japan Society for the Promotion of Science (JSPS), by Grant-in-Aids for Scientific Research (KAKENHI Grant Nos. JP24H00194, JP23K17670, JP22H01168) from JSPS, by Japan Science and Technology Agency (JST) FOREST program (Grant No. JPMJFR222W), by Iketani Science and Technology Foundation (Grant No. 0361078-A), and by The Mitsubishi Foundation (Grant No. 202410051).

## References

- [1] J. Xia *et al.*, Phys. Rev. Lett. **97**, 167002 (2006).
- [2] R. Shimano *et al.*, Nat. Commun. **4**, 1841 (2013).
- [3] B. Huang *et al.*, Nature **546**, 270 (2017).
- [4] M. Weisheit *et al.*, IEEE Trans. Magn. **42**, 3072 (2006).
- [5] X. Chen *et al.*, Measurement **46**, 52 (2013).
- [6] S.-Y. Lin, Y.-K. Liao, and C.-B. Wu, Chin. J. Phys. **55**, 698 (2017).
- [7] A. Ikeda *et al.*, arXiv, 10.48550/arXiv.2509.07383 (2025), to be published in Phys. Rev. Research (DOI: <https://doi.org/10.1103/vy7j-ylb4>).
- [8] A. Ikeda *et al.*, J. Appl. Phys. **136**, 175902 (2024).
- [9] J. Xia *et al.*, Appl. Phys. Lett. **89**, 062508 (2006).
- [10] S. Yamane, *Pmoke - pulsed MOKE measurement CLI*, comp. software, <https://github.com/Kerr-group/pmoke> (visited on 11/30/2025).
- [11] F. Heider, D. J. Dunlop, and N. Sugiura, Science **236**, 1287 (1987).
- [12] Z. Šimša, H. Legall, and P. Široký, Phys. Stat. Solidi B Basic Res. **100**, 665 (1980).
- [13] W. F. J. Fontijn *et al.*, Phys. Rev. B Condens. Matter **56**, 5432 (1997).
- [14] NeoMag, [https://www.neomag.jp/products\\_navi/before\\_catalog.html](https://www.neomag.jp/products_navi/before_catalog.html) (visited on 12/01/2025).
- [15] K. H. J. Buschow, P. G. van Engen, and R. Jongebreur, J. Magn. Magn. Mater. **38**, 1 (1983).
- [16] A. Delin *et al.*, Phys. Rev. B **60**, 14105 (1999).